Unusual events and resonance frequencies in microseismic experiments

J. B. Tary, Department of Physics, University of Alberta
tary@ualberta.ca
and
M. van der Baan, Department of Physics, University of Alberta

GeoConvention 2012:Vision

Summary

Fluid injection to enhance reservoirs permeability is widely used nowadays. Fluid migration is usually monitored by locating the microseismicity induced by the creation or re-activation of fractures. Yet, the total energy due to fluid injection is significantly larger than that released by micro-earthquakes, meaning that other processes in the reservoir must accommodate a part of the total energy (i.e. "silent" deformations must take place). This implies that the total fractured volume may not correspond exactly to the volume of the fluid-induced microseismicity, and more importantly that part of the fluids could migrate out of the reservoir without being noticed. The issues are similar for Carbon Capture and Storage (CCS), where CO2 is carefully injected to not create new fractures, and accurate knowledge of its distribution and location is required for legal reasons. A new approach using continuous passive recordings of the ambient noise would enable to (1) follow any changes in the frequency content over time and (2) detect possible "out-of-band" phenomena of low amplitudes (often below the noise level), which are rejected due to their supposed worthlessness or cannot be recorded by the geophones commonly used during fracturing experiments due to their high or low-frequency content (3000-5000 Hz and 0-5 Hz).

Introduction

A significant part of the energy involved in hydraulic fracturing is not accounted for by the microseismicity [Maxwell et al. (2009)]. This suggests that using only micro-earthquake distributions may not give a reliable description of the deformation occurring inside the reservoir. Indeed, the conventional approach that relies only on triggered events, i.e. discontinuous recordings, with sharp onsets and particular frequency contents (generally >10 Hz) gives an incomplete picture of the geomechanical behavior of the reservoir.

For example, laboratory experiments where recorded and located acoustic emissions produced by the compression of a cylindrical sample with or without the presence of water [Benson et al. (2008), Thompson et al. (2009)] show that the use of continuous recordings permits re-examination of a dataset in order to adapt the event detection strategy. The advantages of using continuous recordings for hydrofracture experiments monitoring are further illustrated by Pettitt et al. (2009) who detect long-lasting phenomena such as resonance frequencies. Pettitt et al. (2009) observe that the seismic noise generated during fluid injection has a specific frequency content going up to 1500Hz. The lines of constant frequency between 500 and 1500 Hz could be related to small, repetitive events. These high-frequency events could correspond to rock deformation by the initiation or re-activation of micro-fractures. Concurrently, they also observe a decrease of the frequency content of the seismic noise that might be related to the coalescence of these micro-fractures and a fault communication between two highly microseismic areas. In this case, only the variation of the frequency content with time revealed this possible fault communication, demonstrating the utility of continuous recordings with an expanded upper frequency bandwidth.

Methodology

The continuous data are first analyzed using different time-frequency transforms (Short-time Fourier Transform - STFT, continuous wavelet transform - CWT, S-transform; Figure 1) [Reine et al. (2009)] to search for modifications in the frequency content of the ambient noise over time. These transforms are particularly appropriate to study the evolution of the frequency content of non-stationary signals. A regular seismic trace is transformed into a spectrogram, function of time and frequency.

The STFT transform is simply obtained by taking the Fourier transform of a windowed signal, and then sliding the window along the complete signal. This transform has a fixed window size whatever the frequency investigated, and hence a fixed time-frequency resolution. Conversely, both the CWT and the S-transform have varying time-frequency resolution, with a window size changing automatically depending on the analyzed frequency. In the case of the S-transform, the size of a Gaussian window is inversely proportional to the analyzed frequency. The CWT uses a particular basis function known as the mother wavelet [Daubechies (1992)]. In this study we use the Morlet wavelet. The window size is not explicitly written in the case of the CWT. A scale factor is used to stretch and squeeze the mother wavelet in the time domain, resulting in a higher frequency and a shorter window for low values of the scale factor. Therefore, for low frequencies, the S- and wavelet transforms has a high frequency resolution but a low time resolution, and vice-versa for high frequencies. The evolution of the frequency content with time will then be included in a comprehensive system together with the microseismicity, “out-of-band” phenomena, and the stages of the experiment (slurry flow) with the intention of producing a new physical model combining all the previously mentioned observations.

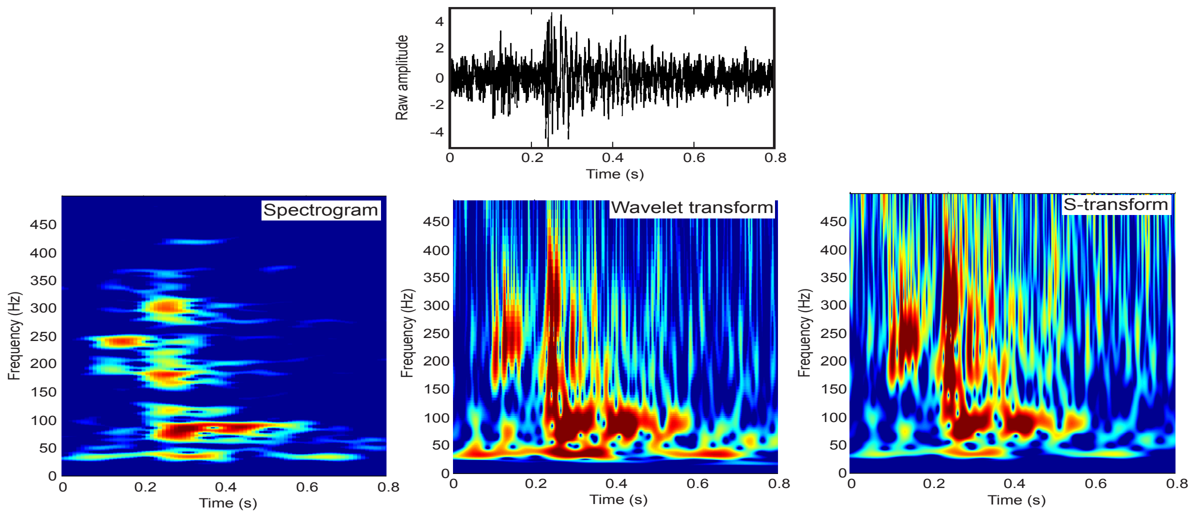

Figure 1 : Spectrogram, S-transform and wavelet transform of the micro-earthquake presented on top. Data courtesy of Husky.

Preliminary analysis

A dataset with continuous recordings, a regular frequency bandwidth and intermediate quality was chosen to test the methodology on real data. Twelve 3-components geophones recorded continuously two fracturing experiments of ∼3 hours each. Regular geophones were used with a sample rate of 4 kHz, giving a frequency bandwidth for the experiment of approximately 10-2000 Hz. During the first stage, the geophones are installed in a deviated borehole (between ∼2140 and ∼2250 m) and spaced by ∼10 m, whereas in the second stage, the geophones are installed in a vertical borehole (between ∼2190 and ∼2300 m) and spaced by ∼10 m. Different injection wells are used, the location of the two stages being approximately 3.4 km apart.

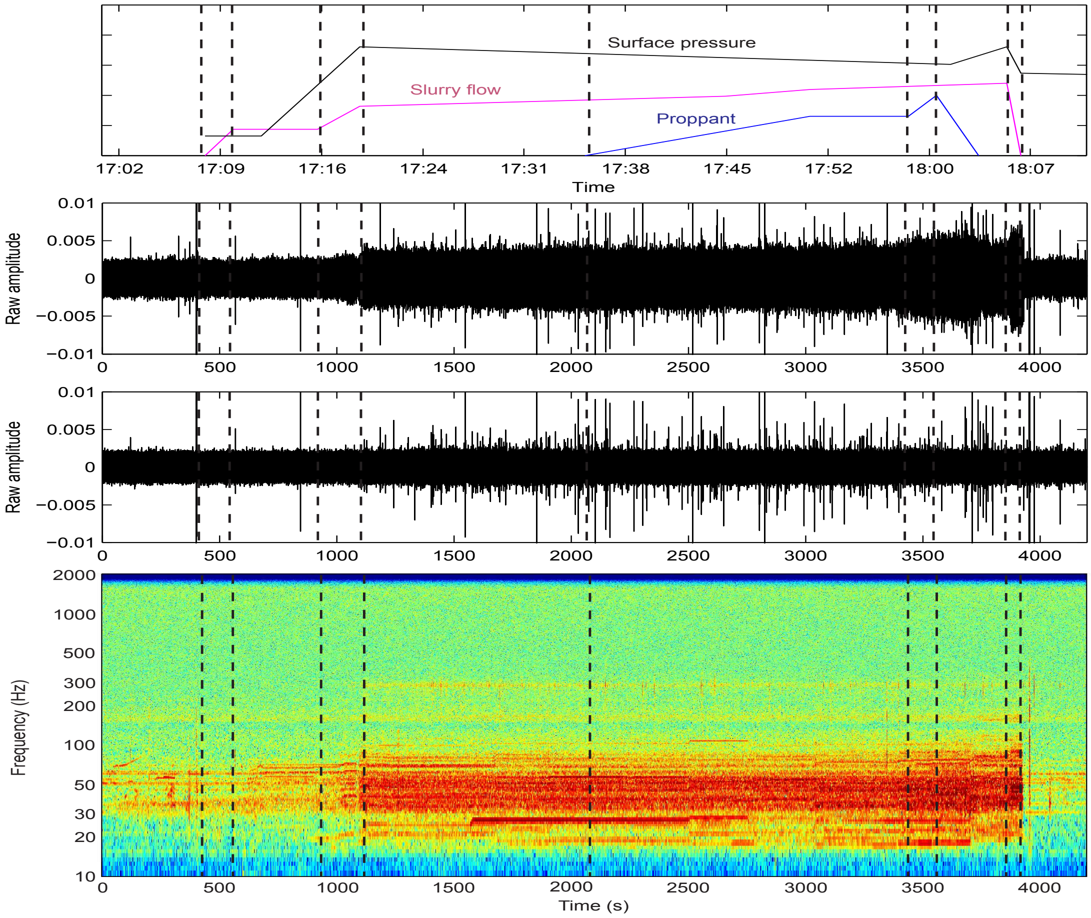

Figure 2 : From top to bottom: (1) evolution of the slurry flow, the proppant concentration and the surface pressure; (2) continuous seismic trace of the vertical component of the deepest geophone (12); (3) same continuous seismic trace band-pass filtered between 100 and 1600 Hz; (4) STFT with a logarithmic scale for the frequency axis. Many events below the noise level are visible on the filtered trace. Steps (at $\sim$1000 s for example), appearance and disappearance of lines of constant frequency (at $\sim$25 Hz between 1500 and 2500 s for example), comma (at $\sim$100 s and $\sim$80 Hz) are visible on the time-frequency representation. These modifications could be related to repetitive failures of micro-fractures at a characteristic frequency or the resonance of fluid-filled fractures of different shapes and sizes. The black dashed lines indicate the time of the main changes of the slurry flow and proppant concentration. Data courtesy of Husky.

Interestingly, during the first analysis of the data, only few micro-earthquakes are detected (22 and 76 events for stage 1 and 2, respectively). This indicates that if not all injected energy is dissipated by brittle failure, then other processes must play a role which may generate unusual events. In a second analysis, after bandpass filtering the data, many more events are detected (350 events; Figure 2). The time-frequency analysis helped greatly in finding appropriate filtering parameters. It also indicates that high noise levels may blanket the microseismicity. Brittle failure may be more dominant in fracturing than anticipated from detected events alone.

To visualize the frequency content of the complete experiment, we chose to use the STFT transform for its fixed time-frequency resolution over the whole frequency range (0-2 kHz), and for its simple formalism allowing to change easily the window length and percentage overlap (Figure 2). A large Hanning window of 1 s, suitable for analysis of frequencies above 2 Hz, with an overlap of 0.2 s is used in order to decrease the computer time necessary to calculate the STFT. We see a clear correlation between the slurry flow, the noise energy and frequency content ($\sim$10-100 Hz). During the experiment, we also observe particular features on the time-frequency representation like the appearance or disappearance of lines of constant frequency, modifications in the frequency of these lines (steps) and a signal with a monotonic frequency content increasing with time (comma-shaped in spectrograms). The comma-shaped signal shows a change very progressive (lasting 125 s) of its frequency content toward higher frequencies (approximately from 70 to 80 Hz).

The presence of lines of constant frequency could result from the generation of repetitive events at a characteristic frequency (i.e. failure of micro-fractures), or from the opening of resonators, that could be fluid-filled fractures, driven by the fluid movements during the experiment. The steps in the characteristic frequency could correspond to a rapid change in the frequency of the repetitive events (from 25 to 30 events/s for example), or a rapid change in the shape and size of the resonator (growing of a fracture, coalescence of micro-fractures). The same mechanisms in a longer time scale could also explain the comma-shaped signal. Although the method is still in development, this example shows clearly the advantages to use continuous recordings to investigate the deformations occurring inside the reservoir.

Conclusions

For moderate-to-poor quality data, energy estimations on the amount of brittle failure may be underestimated since microseismic events may occur but are simply not detected. Here 3.5 times more events are detected after a simple STFT analysis of the continuous signals, allowing to appropriately filter the data. This indicates that more energy may be released due to brittle failure than previously anticipated; yet it cannot explain why injected energy is many orders of magnitude larger than that released by brittle failure [Maxwell et al. (2009)].

Much information is contained in microseismic recordings that are normally not analyzed. In particular, time-frequency analysis may help reveal changes in resonance frequencies, possibly created due to tensile fracturing or semi-brittle or even ductile deformation (e.g., fluid flow along an existing fault). For instance, tensile opening of fractures due to fluid injection and subsequent intrusion of the fluid into the newly generated or augmented fracture is likely to be a subtle effect, not necessarily recognized by a sufficiently strong microseismic event (i.e., brittle failure); yet it may produce a tremor-like signal, recognizable using a time-frequency analysis.

Currently there is a strong emphasis on short turn-around times for microseismic experiments since one of the leading business drivers is the use of event locations to optimize hydraulic fracturing experiments. There is however significant scientific as well as potentially long-term economic advantage in performing more in-depth analyses in the post-processing stage to understand better the interrelationships between chosen injection strategy and actual brittle, semi-brittle and ductile deformation inside the reservoirs. There is thus a strong need for increased observational and theoretical analysis of recorded unusual events, observed resonance frequencies and their potential causes.

Acknowledgments

The authors would like to thank the sponsors of the Microseismic Industry Consortium for financial support, and Husky for permission to show and use their data.

References

Benson, P. M., S. Vinciguerra, P. G. Meredith, and R. P. Young, 2008, Laboratory Simulation of Volcano Seismicity: Science, **322**, 249–252.

Daubechies, I., 1992, Ten lectures on wavelets: Society for Industrial and Applied Mathematics.: Presented at the CBMS-NSF regional conference series in applied mathematics.

Maxwell, S. C., J. Shemeta, E. Campbell, and D. Quirk, 2009, Microseismic Deformation Rate Monitoring: EAGE, Paper A18.

Pettitt, W., J. Reyes-montes, B. Hemmings, E. Hughes, and R. P. Young, 2009, Using Continuous Microseismic Records for Hydrofracture Diagnostics and Mechanics: SEG Expanded Abstract, **28**, 1542–1546.

Reine, C., M. van der Baan, and R. Clark, 2009, The robustness of seismic attenuation measurements using fixed- and variable-window time-frequency transforms: Geophysics, **74**, WA123–WA135.

Thompson, B. D., R. P. Young, and D. A. Lockner, 2009, Premonitory acoustic emissions and stick-slip in natural and smooth-faulted Westerly granite: Journal of Geophysical Research, **114**, 1–14.